

We are IntechOpen, the world's leading publisher of Open Access books Built by scientists, for scientists

6,900

Open access books available

186,000

International authors and editors

200M

Downloads

Our authors are among the

154

Countries delivered to

TOP 1%

most cited scientists

12.2%

Contributors from top 500 universities



WEB OF SCIENCE™

Selection of our books indexed in the Book Citation Index
in Web of Science™ Core Collection (BKCI)

Interested in publishing with us?
Contact book.department@intechopen.com

Numbers displayed above are based on latest data collected.
For more information visit www.intechopen.com



Non-Linear Dielectric Response of Ferroelectrics, Relaxors and Dipolar Glasses

Seweryn Miga¹, Jan Dec¹ and Wolfgang Kleemann²

¹*Institute of Materials Science, University of Silesia, Katowice*

²*Angewandte Physik, Universität Duisburg-Essen, Duisburg*

¹*Poland*

²*Germany*

1. Introduction

The dielectric response of dielectrics with respect to temperature, pressure, frequency and amplitude of the probing electric field is an essential issue in dielectric physics (Jonscher, 1983). This concerns both normal dielectrics and those specified as ferro- or antiferroelectrics (Lines & Glass, 1977). This basic phenomenon of dielectric materials has been extensively studied in the literature both experimentally and theoretically, however, mainly restricting to the linear dielectric response where a linear relationship between polarization, P , and external electric field, E ,

$$P = \varepsilon_0 \chi_1 E, \quad (1)$$

is fulfilled. Here ε_0 and χ_1 stand for the electric permittivity of the free space (dielectric constant) and the linear electric susceptibility of a given dielectric material, respectively. In the framework of this approach the analysis of the dielectric relaxation is possible via the Debye model (including the Cole-Cole equation and related formulae in case of multidisperse behavior) and the relaxation rate can often be described by an Arrhenius relation (Jonscher, 1983; Lines & Glass, 1977; Debye, 1929; von Hippel, 1954; Böttcher, 1973; Kremer & Schönhals, 2003) or by an activated dynamic scaling law (Fisher, 1986; Kleemann et al., 2002) which in the particular case of the exponent $\theta\nu = 1$ converts into the well known Vogel-Fulcher-Tammann relation (Jonscher, 1983; Kremer & Schönhals, 2003). More complex distribution functions of relaxation-times are used as well (Jonscher, 1983; Böttcher, 1973; Kremer & Schönhals, 2003).

At higher electric fields E , (1) becomes violated and the relation between polarization and electric field is better represented by a power series of E ,

$$P = \varepsilon_0 (\chi_1 E + \chi_2 E^2 + \chi_3 E^3 + \chi_4 E^4 + \chi_5 E^5 + \dots), \quad (2)$$

which contains higher order terms with respect to the external electric field, where χ_i with $i > 1$ are the non-linear susceptibilities: second-order, third-order and so on (Böttcher, 1973). These non-linear components are referred to as hypersusceptibilities and the non-linear contribution to the polarization response is designated as the hyperpolarization (Jonscher,

1983). While the higher-order susceptibilities contain a wealth of important information (Wei & Yao, 2006a; Wei & Yao, 2006b), the hyperpolarization has nevertheless been less studied due to obstacles like (i) the difficulty of the respective dielectric measurements, because the nonlinear signal is usually some orders of magnitude smaller than the linear response, and (ii) lack of an appropriate theory to deal with dielectric spectra as a function of the electric field (Chen & Zhi, 2004).

In order to overcome the technological challenge we have constructed a fully automatized *ac* susceptometer for simultaneous measurements of the phase resolved complex linear and complex non-linear *ac* susceptibilities of lossy and dispersive dielectric materials (Miga, Dec & Kleemann, 2007). It allows measurements over a wide range of experimental variables, such as *ac* amplitudes up to 40 V, frequencies from 10^{-2} to 10^3 Hz, and temperatures from 100 K to 600 K utilizing only current/voltage and analogue/digital converters and a computer. In contrast to the commonly used analysis of the charge accumulated on a standard capacitor in series with the sample our method is based on the analysis of the current flowing directly through the sample. Absence of any capacitive voltage dividers in the measurement circuit eliminates uncontrolled phase shifts. That is why the instrument provides high quality nonlinear susceptibility data and in particular appears as a very convenient tool for discrimination between continuous and discontinuous phase transitions when determining the sign of the real part of the third order dielectric susceptibility.

We have applied this new instrument to various basic ferroelectric scenarios, such as the classic first- and second-order ferroelectric transitions of barium titanate (BaTiO_3) (Miga & Dec, 2008), triglycine sulphate (TGS) (Miga & Dec, 2008) and lead germanate ($\text{Pb}_5\text{Ge}_3\text{O}_{11}$) (Miga & Dec, 2008), the double anomalous second-order transitions of Rochelle salt (Miga et al., 2010a), the smeared transition of the classic relaxor ferroelectrics lead magno-niobate ($\text{PbMg}_{1/3}\text{Nb}_{2/3}\text{O}_3$, PMN) (Dec et al., 2008) and strontium-barium niobate ($\text{Sr}_{0.61}\text{Ba}_{0.39}\text{Nb}_2\text{O}_6$, SBN61) (Miga & Dec, 2008), the dipolar glassy and ferroelectric transitions of Li^+ -doped potassium tantalate ($\text{K}_{1-x}\text{Li}_x\text{TaO}_3$, KLT) with $x = 0.005, 0.011$ and 0.063 (Dec et al., 2010; Miga et al., 2010b).

2. Theoretical background of nonlinear dielectric response

Dielectric properties of materials are usually investigated via linear dielectric response. In this case a linear relationship, Eq. (1), between polarization, P , and external electric field, E , is fulfilled. At higher field intensities, the polarization may be a non-linear function of the electric field strength. For not too high electric field strength, one can present the polarization as the power series expansion in the variable E , Eq. (2). For symmetry reasons the second-order dielectric susceptibility is nonzero only for macroscopically noncentrosymmetric systems.

Let us consider the Landau-Ginzburg-Devonshire (LGD) theory of ferroelectric phase transitions (PT) (Ginzburg, 1945; Devonshire, 1949). According to this theory the free energy density G of a ferroelectric material within its paraelectric phase is represented as a power series expansion with respect to the polarization P ,

$$G(E, P, T) = -EP + G_0 + \frac{1}{2}A(T - T_0)P^2 + \frac{1}{4}BP^4 + \frac{1}{6}CP^6 + \dots \quad (3)$$

where G_0 stands for the free energy at $P = 0$, A and T_0 are constants. B and C are usually smooth functions of temperature (Fujimoto, 2003). In the ferroelectric phase the polarization P , yields the spontaneous one, P_s , as an order parameter. The sign of B determines the kind of the PT. For positive B a continuous (second-order) PT occurs. On the other hand, for negative B a discontinuous (first-order) PT appears. Let us first consider a continuous PT to occur at $T_0 = T_c$. In this case one can drop the last term in Eq. (3) without loss of generality. Thermodynamic equilibrium requires fulfilment of the condition

$$\frac{\partial G}{\partial P} = 0 = -E + A(T - T_c)P + BP^3. \quad (4)$$

This relationship between E and P denotes the electric equation of state. After successive differentiation of this equation with respect to P one obtains the following susceptibilities (Ikeda et al., 1987):

$$\chi_1 = \frac{1}{\epsilon_0[A(T - T_c) + 3BP^2]} \quad (5)$$

$$\chi_2 = -3\epsilon_0^2 BP \chi_1^3 \quad (6)$$

$$\chi_3 = -(1 - 18\epsilon_0 BP^2 \chi_1) \epsilon_0^3 B \chi_1^4. \quad (7)$$

The second-order susceptibility is proportional to the polarization P , therefore it changes sign when the polarization changes direction. Additionally χ_2 vanishes when the polarization of the sample vanishes. That is why χ_2 is a sensitive probe of the net polarization, but it is unsuitable for determination of the PT order. In contrast to χ_2 the odd order susceptibilities χ_1 and χ_3 depend on the square of the polarization, which makes them insensitive to the orientation of the polarization. Moreover, χ_1 and χ_3 do not vanish, even if the polarization is equal to zero. For classic ferroelectrics on heating the spontaneous polarization P_s vanishes at the PT point and is zero within the paraelectric phase, where Eq. (7) simplifies to

$$\chi_3 = -\epsilon_0^3 B \chi_1^4. \quad (8)$$

Due to positive B , χ_3 is negative above a continuous PT point. Within the ferroelectric phase $P = P_s$ and $P_s^2 = (A/B)(T_c - T)$, hence,

$$\chi_3 = 8\epsilon_0^3 B \chi_1^4. \quad (9)$$

Within the ferroelectric phase χ_3 has a positive sign. Thus the LDG theory predicts a change of sign of χ_3 at a continuous PT. The scaling theory (Stanley, 1971) predicts that B scales as $B = B_0 |\tau|^{\gamma - 2\beta}$, where $\tau = (T - T_c)/T_c$. γ and β are critical exponents of the linear susceptibility and of the order parameter, respectively. For the Landau universality class, where $\gamma - 2\beta = 0$ (i. e. $\gamma = 1$, $\beta = 1/2$) one expects a temperature independent value of B within the paraelectric phase.

A similar calculation for a discontinuous PTs, where $B < 0$ and $C > 0$, yields $\chi_3 > 0$ at all temperatures, in particular also above PT (Ikeda et al., 1987). Fortunately from an

experimental point of view χ_3 is given by this same equation (8) within paraelectric phase independent of the ferroelectric PT order. The sign of χ_3 is a sensitive probe for discrimination between continuous and discontinuous ferroelectric PTs.

In all known ferroelectrics the paraelectric phase is located above the stability range of the ferroelectric one. However, sodium potassium tartrate tetrahydrate (Rochelle salt, RS) (Valasek, 1920, 1921) apart from a classic high temperature paraelectric phase has an additional, unusual one located below the ferroelectric phase. Both PTs, between the paraelectric phases and the ferroelectric one have continuous character. In order to predict the sign of χ_3 within the low-temperature paraelectric phase one can refer to the theory of Mitsui (Mitsui, 1958). Within this theory the electric equation of state for RS is similar to Eq. (4) with a positive coefficient of the cubic term, P^3 . Therefore a negative sign of χ_3 is expected within low-temperature paraelectric phase (Miga et al., 2010a).

Another class of dielectrics are relaxor ferroelectrics. They are usually considered as structurally disordered polar materials, which are characterized by the occurrence of polar nanoregions (PNRs) of variant size below the so-called Burns temperature, T_d (Burns & Dacol, 1983) far above the ferroelectric Curie temperature, T_c . In contrast to conventional ferroelectrics, relaxors do not exhibit any spontaneous macroscopic symmetry breaking. In addition they are characterized by a large, broad and frequency-dependent peak in the temperature dependence of dielectric susceptibility. According to the spherical random-bond-random-field (SRBRF) model (Pirc & Blinc, 1999) the dipole moments of individual nanopolar clusters interact via a spin-glass-type random exchange coupling, and are subject to quenched random local electric fields. The model Hamiltonian of such a system is formally written as

$$H = -\frac{1}{2} \sum_{ij} J_{ij} \vec{S}_i \cdot \vec{S}_j - \sum_i \vec{h}_i \cdot \vec{S}_i - g \vec{E} \cdot \sum_i \vec{S}_i, \quad (10)$$

where J_{ij} are glass-like random intercluster couplings or bonds, \vec{h}_i and \vec{E} random local and uniform external electric fields, respectively. In the dynamic approximation it is assumed that PNRs reorient by means of stochastic flips described by a relaxation time τ . This model yields negative χ_3 with two extremes observed at the freezing temperature, T_f , and at the peak temperature of χ_1 , T_m .

The measured values of χ_1 and χ_3 can be used for calculating the so-called scaled non-linear susceptibility, a_3 , which is given by (Pirc & Blinc, 1999)

$$a_3 = -\frac{1}{\epsilon_0^3} \frac{\chi_3}{\chi_1^4}. \quad (11)$$

Within the paraelectric phase of classic ferroelectrics a_3 is equal to the nonlinearity coefficient B , cf. Eqs. (8) and (11). For ferroelectrics displaying a continuous PT, $a_3 = -8B$ within ferroelectric phase. The SRBRF model yields negative χ_3 and positive a_3 with two extremes observed at the freezing temperature, T_f , and at the peak temperature of χ_1 , T_m . It should be noticed that systems like dipolar glasses a_3 are also expected to exhibit a critical singularity at T_f , where $\chi_3 \propto (T - T_f)^{-\gamma}$ with the mean field exponent $\gamma = 1$ (Pirc et al., 1994).

A schematic comparison of predictions of the above theories is presented in Fig. 1.

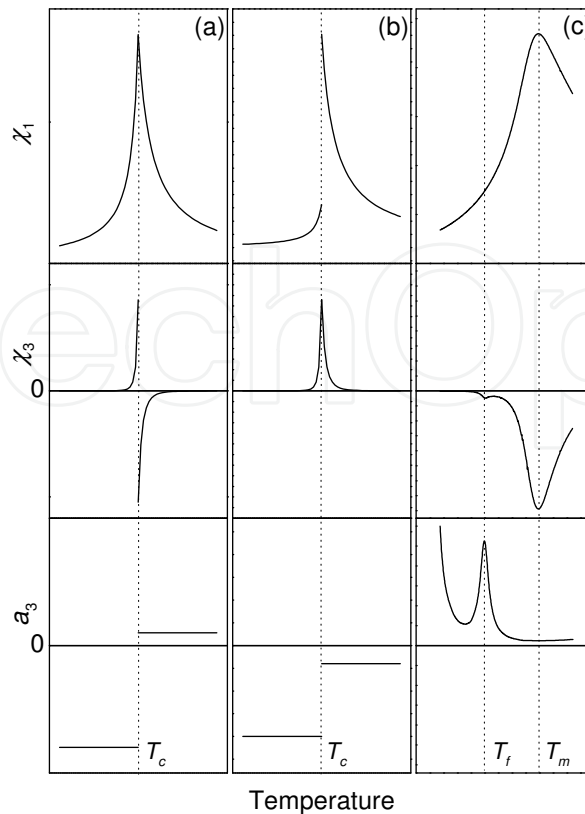


Fig. 1. Schematic presentation of linear and nonlinear responses of classic ferroelectrics with (a) continuous PTs, (b) discontinuous PTs, and (c) relaxor ferroelectrics (see text).

3. Methods of measurement of nonlinear dielectric response

Nonlinear dielectric response can be measured using two different kinds of experimental methods. The first one is based on the investigation of the *ac* linear dielectric susceptibility as a function of a *dc* bias field. A schematic presentation of this method is shown in Fig. 2a. One applies to the sample a weak probing *ac* electric field with fixed amplitude (that warrants a linear response) and a superimposed variable *dc* bias field, E_B . The bias field amplitude may reach values up to $5.5 \cdot 10^7 \text{ Vm}^{-1}$ (Leont'ev et al., 2003). In barium titanate a strong *dc* field induces the PT between paraelectric and ferroelectric phases (Wang et al., 2006). By changing the value of the *dc* electric field the local slope of the polarization curve is probed in many points. For such a kind of experiment one can use commercially available LRC meters or impedance analyzers, e.g. Agilent E4980A or Solartron 1260. The electric field dependence of the linear susceptibility of ferroelectrics displaying continuous PT fulfils the following relations (Mierzwa et al., 1998):

$$\frac{1}{\chi^3(E)} + \frac{3}{\chi^2(E)\chi(0)} - \frac{4}{\chi^3(0)} = 27\epsilon_0^3 B E^2 \quad (12)$$

for the paraelectric phase and

$$\frac{1}{\chi^3(E)} - \frac{3}{2\chi^2(E)\chi(0)} + \frac{1}{2\chi^3(0)} = 27\epsilon_0^3 B E^2 \quad (13)$$

for the ferroelectric one. $\chi(E)$ and $\chi(0)$ are the susceptibilities for bias, E , and zero electric field, respectively. By use of Eqs. (12) and (13) one can calculate the nonlinearity coefficient B . Its knowledge allows us to calculate the third-order nonlinear susceptibility χ_3 . Unfortunately, the above described method has at least one restriction when investigating the nonlinear dielectric response. Namely, during so-called field heating/cooling runs, unwanted poling and remnant polarization of the investigated sample can evolve under a high bias field.

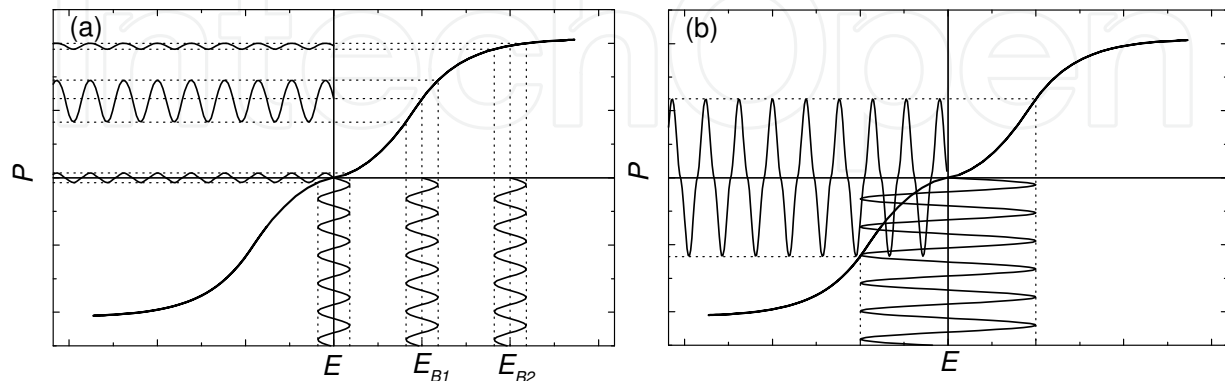


Fig. 2. Presentation of methods of measurement of nonlinear dielectric response using (a) a weak probing *ac* electric field with fixed amplitude and a superimposed variable *dc* bias field, and (b) an enhanced *ac* field. The effects are exaggerated for visualisation.

The second kind of method is free from this restriction. A schematic presentation of this method is shown in Fig. 2b. During the experiment the sample is exposed to an *ac* probing field with sufficiently large amplitude. Consequently, under this condition the temperature dependences of the linear and nonlinear susceptibilities are determined under zero *dc* field in heating and cooling runs. That is why the nonlinear susceptibility detected this way can be referred to as a dynamic nonlinear susceptibility related to *ac* dielectric nonlinearity. Usually the amplitude of this field is much smaller than the bias field strength used in the above described experiment. As a result of the nonlinear $P(E)$ dependence, the output no longer remains harmonic. The distorted signal may be subjected to Fourier analysis revealing all harmonic components in the polarization response. This is the main idea of our nonlinear *ac* susceptometer (Miga et al., 2007). Using harmonics of displacement current density j_i one can calculate the linear and nonlinear dielectric susceptibilities χ_i as follows:

$$\begin{aligned}
 \chi_1 &= \frac{1}{\varepsilon_0 \omega} E_0^{-1} (j_1 + j_3 + j_5 + j_7) - 1, \\
 \chi_2 &= \frac{1}{\varepsilon_0 \omega} E_0^{-2} (j_2 + 2j_4 - 3j_6), \\
 \chi_3 &= \frac{1}{\varepsilon_0 \omega} E_0^{-3} \left(-\frac{4}{3}j_3 - 4j_5 - 8j_7 \right), \\
 \chi_4 &= \frac{1}{\varepsilon_0 \omega} E_0^{-4} (-2j_4 + 8j_6), \\
 \chi_5 &= \frac{1}{\varepsilon_0 \omega} E_0^{-5} \left(\frac{16}{5}j_5 + 16j_7 \right)
 \end{aligned} \tag{14}$$

where ω and E_0 are the angular frequency and the amplitude of the applied electric field respectively. In Eq. 14 the terms up to seventh order are involved, hence, susceptibilities up to the fifth order can be regarded as reliable even for strongly nonlinear materials. Neglecting harmonics higher than the order of a considered susceptibility may lead to artificial effects. The next important point is the simultaneous measurement of all displacement current components, which considerably improves the accuracy of the measured susceptibilities (Bobnar et al., 2000). In case that the phase shifts of the displacement current harmonics are known it is possible to calculate the real, χ'_i , and imaginary, χ''_i , parts of all susceptibilities. This is impossible, when measurements are done with a *dc* bias electric field. It should be noted that up to now commercial instruments for the dynamic measurement of complex nonlinear dielectric susceptibilities are unavailable.

4. Experimental results

4.1 Ferroelectrics displaying continuous PTs

Triglycine sulphate, $(\text{NH}_2\text{CH}_2\text{COOH})_3\cdot\text{H}_2\text{SO}_4$ (TGS) is a model ferroelectric displaying a continuous PT. Sodium potassium tartrate tetrahydrate (Rochelle salt, RS), $\text{NaKC}_4\text{H}_4\text{O}_6\cdot 4\text{H}_2\text{O}$, and lead germanate, $\text{Pb}_5\text{Ge}_3\text{O}_{11}$ (LGO) exhibit continuous PTs, as well. Despite the quite different structures of the crystals and different mechanisms of their PTs, a negative sign of the real part of the third-order nonlinear susceptibility is expected in their paraelectric phases. Fig. 3 shows the temperature dependences of the real parts of the linear, the third order nonlinear dielectric susceptibilities, and the scaled susceptibility, a_3 . The linear susceptibility of a TGS crystal (Fig. 3a) obeys a Curie-Weiss law within the paraelectric phase very well with a critical exponent $\gamma = 1.000 \pm 0.006$. According to predictions of the phenomenological theory of ferroelectric PT, χ'_3 changes its sign at the PT point (Fig. 3b).

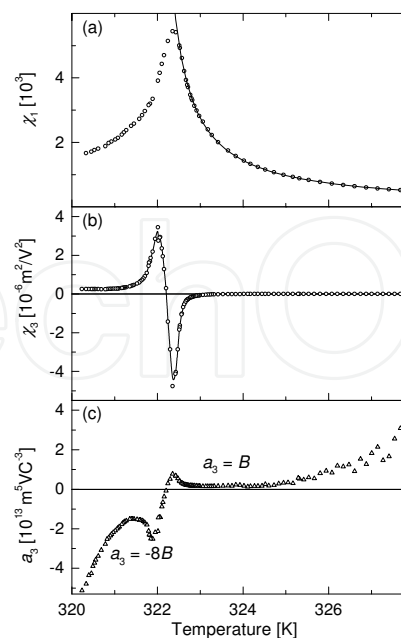


Fig. 3. Temperature dependences of the real parts of the linear (a) and third order non-linear (b) susceptibilities and a_3 coefficient (c) of TGS. The amplitude of the probing *ac* electric field was $5\text{kV}\cdot\text{m}^{-1}$.

While below T_c the third-order susceptibility has positive values, it is negative above T_c . As was mentioned earlier such change in the sign of χ_3' is one of the primary features of the continuous ferroelectric PT. The scaled non-linear susceptibility has been evaluated using Eq. (11). The measured values of χ_1' and χ_3' were used for calculations. The temperature dependence of a_3 of TGS crystal is shown in Fig. 3c. Within the paraelectric phase a_3 is equal to B and has a positive value. This is an attribute of the continuous PT. Moreover, a_3 is practically temperature independent within the temperature range of $T_c + 0.2 \text{ K} < T < T_c + 2 \text{ K}$ above the PT point. This behaviour is consistent with predictions of the scaling theory and confirms that TGS belongs to the Landau universality class. Weak temperature dependence of a_3 and $1/|T-T_c|$ dependence of χ_1' leads to a $1/|T-T_c|^4$ anomaly of χ_3' (see Eq. 11). Therefore the temperature dependence of χ_3' is much sharper than that of χ_1' . Consequently, χ_3' rapidly vanishes in the surrounding of the PT. An increase of a_3 as observed within the paraelectric phase close to T_c is probably due to crystal defects. A similar effect was reported for a γ -ray damaged TGS crystal (Cach, 1988). Then within the ferroelectric phase a_3 changes slowly due to the contribution of the domain walls to the resultant dielectric response. In the ferroelectric state the measured values of the linear and non-linear susceptibilities, which were used for calculation, involved the responses not only from the "pure" ferroelectric system but also from the domain walls, which were forced to move under the probing electric field.

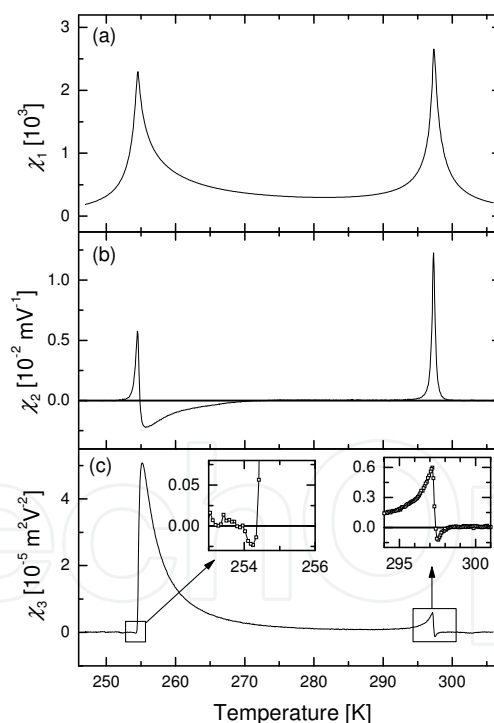


Fig. 4. Temperature dependences of the real parts of the linear (a), the second (b) and the third (c) order nonlinear susceptibilities of Rochelle salt. The amplitude of the probing ac electric field was 500 Vm^{-1} .

Fig. 4 shows the temperature dependences of the linear, the second, and the third-order nonlinear susceptibilities of Rochelle salt. The temperature dependences of χ_1' and χ_3' are, close to the high temperature ferroelectric-paraelectric PT ($\approx 297.4 \text{ K}$), qualitatively similar to

those of the TGS crystal. As was mentioned earlier, RS displays an additional low temperature PT. This transition between the ferroelectric and the low temperature paraelectric phase appears at about 254.5 K. At this PT χ_3' changes its sign as compared to the high temperature PT (Fig. 4c). As a result of the inverse order of phases, χ_3' is negative below and positive above the low temperature PT. In this way the third-order nonlinear susceptibility is negative in both paraelectric phases close to PT points. Fig. 4b shows the temperature dependence of the second-order nonlinear susceptibility. The sign of this susceptibility depends on the net polarization orientation. Therefore it can be changed by polarization of the sample in the opposite direction. The simplest way to change the sign of χ_2' is a change of the wires connecting the sample to the measuring setup. So, in contrast to sign of the χ_3' , the sign of the second order nonlinear susceptibility is not very important. In the case of χ_2' most important is its nonzero value and the observed change of sign of this susceptibility at 273 K. This hints at a modification of the domain structure within the ferroelectric phase. The next change of sign at the low temperature PT point is originating from different sources of the net polarization above and below this point. Above 254.5 K this polarization comes from the uncompensated ferroelectric domain structure, whereas within the low-temperature paraelectric phase it originates merely from charges screening the spontaneous polarization within the ferroelectric phase.

Lead germanate (LGO) displays all peculiarities of a continuous ferroelectric PT (see Fig. 5 a, c, e) (Miga et al., 2006). However, a small amount of barium dopant changes this scenario (Miga et al., 2008). Ba^{2+} ions replacing the host Pb^{2+} influence the dielectric properties. 2% of barium dopant causes a decrease of the linear susceptibility, broadening of the temperature dependence of χ_1' , and a decrease of the PT temperature. Despite all these changes the temperature dependences of χ_1' for pure and barium doped LGO are qualitatively similar. A completely different situation occurs, when one inspects the nonlinear dielectric response. Small amounts of barium dopants radically change the temperature dependence of the third-order nonlinear susceptibility (Fig.5 b). Similarly to linear one the anomaly of the third-order nonlinear susceptibility shifts towards lower temperature and decreases. The most important difference is the lacking change of sign of χ_3' . In contrast to pure LGO for barium doped LGO the third-order nonlinear susceptibility is positive in the whole temperature range. Therefore one of the main signatures of classic continuous ferroelectric PTs is absent. Due to the positive value of χ_3' the scaled nonlinear susceptibility is negative in the whole temperature range (Fig. 5d). No change of a_3 is observed. This example shows the high sensitivity of the nonlinear dielectric response to the character of the PT. In the discussed case a change of character of the PT is due to the presence of barium induced polar nanoregions (PNRs). The occurrence of PNRs results in weak relaxor properties of barium doped LGO.

4.2 Ferroelectrics displaying discontinuous PT

Barium titanate, BaTiO_3 (BT), is a model ferroelectric displaying three discontinuous ferroelectric PTs (von Hippel, 1950). Two of them appear – at rising temperatures - between rhombohedral, orthorhombic and tetragonal ferroelectric phases at about 200 K and 280 K respectively. The final discontinuous PT appears between the ferroelectric tetragonal and the cubic paraelectric phase at about 400 K. Fig. 6 shows the temperature dependences of the real parts of the linear (a) and third-order nonlinear (b) susceptibilities, and the a_3 coefficient (c) of a BT crystal in the vicinity of the ferroelectric-paraelectric PT. The amplitude of a probing ac electric field was equal to 7.5 kV m^{-1} .

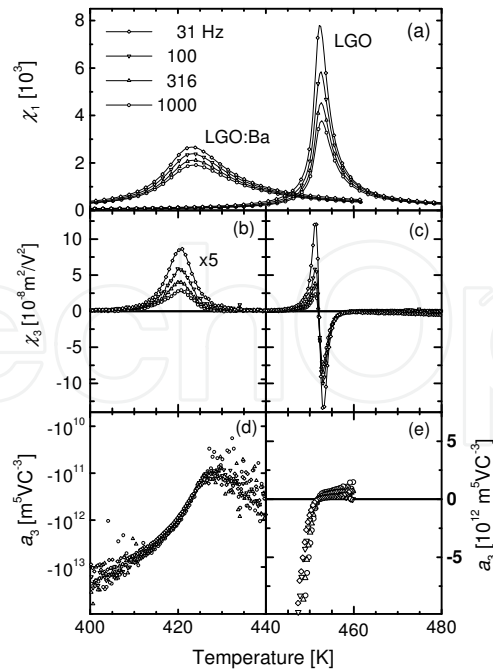


Fig. 5. Temperature dependences of the real part of the linear dielectric susceptibility (a) for LGO:Ba 2% and LGO, real part of third-order nonlinear dielectric susceptibility for (b) LGO:Ba 2% and (c) LGO, and scaled nonlinear susceptibility a_3 for (d) LGO:Ba 2%, and (e) LGO crystals. The amplitude of the probing ac electric field was 15 kV m^{-1} .

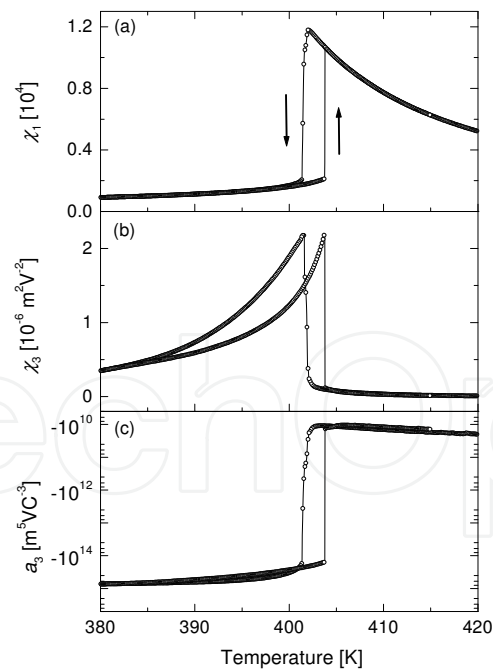


Fig. 6. Temperature dependences of the real parts of the linear (a) and third order non-linear (b) susceptibilities and of the a_3 coefficient (c) of a BaTiO_3 crystal. The amplitude of the probing ac electric field was 7.5 kV m^{-1} .

Temperature hysteresis is one of the typical features of discontinuous PT. Therefore for viewing this phenomenon Fig. 6 presents results for cooling and heating runs. The third-

order nonlinear susceptibility is positive, both within the ferroelectric and the paraelectric phases (Fig. 6b). Just below T_c a rapid decrease of the third-order dielectric susceptibility is observed. For that reason, the value of χ_3' is much smaller within the paraelectric phase than in the ferroelectric one, yet it is still positive. The positive sign of χ_3' as detected in BT is consistent with predictions of the phenomenological theory of discontinuous ferroelectric PTs. Unlike the scaled nonlinear susceptibilities of crystals displaying a continuous PT, a_3 of BaTiO₃ is negative in the whole investigated temperature range (Fig. 6c). However, similarly to TGS (Fig. 3) or RS (Fig. 4) a jump-like change of a_3 occurs at the PT. Within the paraelectric phase a_3 is equal to B (see section 4.1) and displays weak temperature dependence. Wang *et al.* (Wang *et al.*, 2007) proposed incorporation of higher order terms (up to the eighth power) in the Landau potential for the temperature independence of the experimentally obtained B coefficient. This proposition was given for analyzing the data collected with a bias field up to 1500 kV/m. Fig. 6 shows data collected for a two hundred times smaller electric field, for which terms at such high order are not important. They cannot explain the temperature dependence of the nonlinearity coefficient B . Hence, although the nonlinear properties of BaTiO₃ have been investigated already for six decades, the question of the temperature dependence of the nonlinearity parameter B is still open.

4.3 Relaxor ferroelectrics

The classic relaxor ferroelectric lead magno-niobate (PbMg_{1/3}Nb_{2/3}O₃, PMN) (Smolenskii *et al.*, 1960) displays an average cubic structure in the whole temperature range (Bonneau *et al.*, 1991). No spontaneous macroscopic symmetry breaking is observed in this relaxor. On the other hand and in contrast to PMN, the relaxor strontium-barium niobate Sr_{0.61}Ba_{0.39}Nb₂O₆ (SBN61) spontaneously undergoes a structural phase transition. On cooling the vanishing of a mirror plane leads to a lowering of the tetragonal symmetry from $4/mmm$ to $4mm$ at a temperature of about 348 K (Oliver *et al.*, 1988).

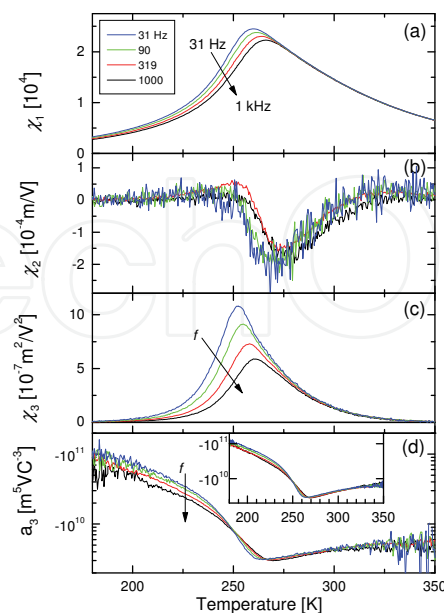


Fig. 7. Temperature dependences of χ_1' (a), χ_2' (b), χ_3' (c) and a_3 (d) of a PMN crystal measured at $f = 31, 100, 319,$ and 1000 Hz. A probing ac electric field with an amplitude of 12 kV/m was applied along the [100] direction.

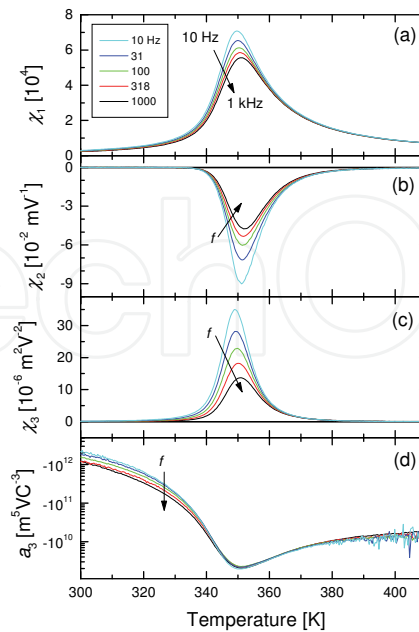


Fig. 8. Temperature dependences of χ_1' (a), χ_2' (b), χ_3' (c) and a_3 (d) of a SBN61 crystal measured at $f = 10, 31, 100, 318,$ and 1000 Hz. A probing ac electric field with an amplitude of 7.5 kV/m was applied along the $[001]$ direction.

Fig. 7 presents the temperature dependences of the real parts of the linear, χ_1' (a), second-order, χ_2' (b), and third-order, χ_3' (c), dielectric susceptibilities and of the scaled nonlinear susceptibility a_3 (d) of the PMN single crystal recorded along $[100]$ direction (Dec et al., 2008). The linear susceptibility displays features of a relaxor i.e. a large, broad and frequency-dependent peak in the temperature dependence. Nonzero χ_2' as presented in Fig. 7b is an indicator of net polarization of the crystal. The presence of this polarization was independently confirmed by measurements of thermo-stimulated pyroelectric current of an unpoled sample. Integration of this current indicates an approximate value of the average polarization as low as 3×10^{-5} C/m². This polarization is much smaller than the spontaneous polarization of ferroelectrics, but is well detectable. The observed pyroelectric response and nonzero χ_2' hints at an incomplete averaging to zero of the total polarization of the PNR subsystem. Fig. 7c shows the temperature dependence of the third-order nonlinear susceptibility. In contrast to the predictions of the SRBRF model, χ_3' is positive in the whole temperature range. The positive sign of χ_3' may result from a term $18\epsilon_0 B P^2 \chi_1$ exceeding unity in Eq. 7. Positive sign of χ_3' results in a negative sign of a_3 . Consequently the sign of a_3 differs from that predicted by the SRBRF model. Having in mind that corrections due to the fifth harmonic contribution produce large noise at temperatures below 210 K and above 310 K (Fig. 7d, main panel), less noisy a_3 data calculated only from first and third harmonics are presented in the inset to Fig. 7d. Since both χ_1' and χ_3' do not display any anomalies in the vicinity of the freezing temperature $T_f \approx 220$ K, also a_3 does not exhibit any maximum in contrast to SRBRF model predictions. It continues to increase monotonically by almost two orders of magnitude when decreasing the temperature from 260 to 180 K. This result is independent of the number of harmonics used for experimental data analysis. It is worth stressing that despite the remarkable

dispersion of χ_1' and χ_3' , the scaled susceptibility a_3 does not display any sizable frequency dependence, even around the temperatures of the susceptibility peaks. It may, hence, be considered as a static quantity (Glazounov & Tagantsev, 2000). According to our result the dispersion of a_3 is even weaker than reported previously (Glazounov & Tagantsev, 2000).

Fig. 8 shows results of measurements of the linear and nonlinear dielectric response of SBN61 crystal (Miga & Dec, 2008). The probing electric *ac* field was applied along [001], which is the direction of the polar axis below T_c . The peak temperatures of the linear susceptibility (Fig. 8a) are a few degrees above the temperature of the structural phase transition. Fig. 8b presents the temperature dependence of the second-order susceptibility. Similarly to results obtained on PMN this susceptibility is non-vanishing. However, the values of χ_2' of SBN61 are almost two orders of magnitude larger than those measured on PMN. Therefore χ_2' is detectable even forty degrees above T_c . Analysis of the thermally stimulated current indicates a net polarization of a nominally unpoled SBN61 crystal equal to 5×10^{-2} C/m². The higher value of this polarization (in comparison with PMN) results in higher values of χ_2' . Fig. 8c shows the temperature dependence of χ_3' . This susceptibility is positive within both the ferroelectric and the paraelectric phase. Again, the sign of χ_3' disagrees with predictions of the SRBRF model. As was discussed above, the positive sign of χ_3' presumably originates from the presence of net polarization (detected by χ_2' , see Fig. 8b). The disagreeing sign of χ_3' leads to a disagreement of the sign of a_3 as well (Fig. 8d). The scaled nonlinear susceptibility shows an anomaly related to the phase transition, but it does not exhibit any additional peak as predicted by the SRBRF model.

The results obtained for both relaxor ferroelectrics are qualitatively similar. Therefore, they are independent of the presence or absence of a structural phase transition and macroscopic symmetry breaking. As discussed in Section 2 the dielectric properties of relaxors are mainly determined by PNRs, which were detected in both of the above relaxors. Unfortunately, the early version of the SRBRF model (Pirc et al., 1994) predicts a negative sign of the third-order nonlinear dielectric susceptibility, which is not confirmed in experiments. Consequently the sign of the scaled nonlinear susceptibility a_3 is incorrect as well. Very probably this unexpected result is due to the fact that the PNRs primary do not flip under the *ac* electric field, but merely change their shape and shift their centers of gravity in the sense of a breathing mode (Kleemann et al., 2011).

4.4 Dipolar glasses

4.4.1 Orientational glasses

The formation of dipolar glasses in incipient ferroelectrics with perovskite structure, ABO_3 , such as $SrTiO_3$ and $KTaO_3$, by *A*-site substitution with small cations at low concentrations has been a fruitful topic since more than 20 years (Vugmeister & Glinchuk, 1990). For a long time probably the best-known example has been the impurity system $K_{1-x}Li_xTaO_3$ (KLT for short) with $x \ll 1$, whose complex polar behavior is known to be due to the interaction of the (nearly) softened transverse-optic mode of the host-lattice and the impurity dynamics (Höchli et al., 1990). Fig. 9 shows the structure model of *A*-site substituted Li^+ viewing the nearest neighbor environment in the $KTaO_3$ lattice from two different perspectives. At very low concentrations, $x \approx 0.01$, it reveals signatures of glasslike behavior (Höchli, 1982; Wickenhöfer et al., 1991), while a ferroelectric ground state with inherent domain structure is encountered at higher concentrations, $x \geq 0.022$ (Kleemann et al., 1987).

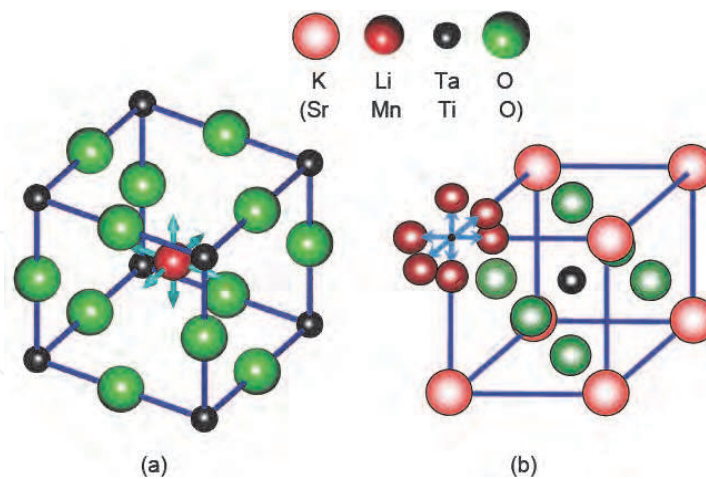


Fig. 9. Displacement vectors (blue arrows) of an off-center Li^+ (Mn^{2+}) ion in *A*-site doped KTaO_3 (SrTiO_3) viewed (a) from the center of 12 surrounding oxygen ions and (b) from the corner of the elementary cell.

Only recently a similar system has been discovered with qualitatively new properties. The impurity system $\text{Sr}_{1-x}\text{Mn}_x\text{TiO}_3$ (SMnT for short; Fig. 9) reveals very similar dipolar glassy properties, but the additional magnetic degrees of freedom of the Mn^{2+} dopant enable simultaneously a spin glass state (Shvartsman et al., 2008). This unique 'multiglass' situation has paved the way to a new materials class: 'disordered multiferroics' (Kleemann et al., 2008). In addition to conventional tests of the glass transition, *e. g.* by verifying the divergence of the polar relaxation times, the behavior of the nonlinear susceptibility is believed to similarly decisive. As was first acknowledged in spin glass physics (Binder & Young, 1986), but later on also in the field of orientational glasses (Binder & Reger, 1992), criticality at the glass temperature, T_g , is expected to give rise to a divergence of the third-order nonlinear susceptibility, $\chi_3' \propto \partial^3 P / \partial E^3$, where the polarization P denotes the homogeneous order parameter. Recent experimental attempts will be reported below.

4.4.2 Orientational glass $\text{K}_{0.989}\text{Li}_{0.011}\text{TaO}_3$

The experiments on KLT were performed on a Czochralski grown single crystal sample with $x = 0.011$ with dimensions $3 \times 2 \times 0.5 \text{ mm}^3$ and (100) surfaces (Kleemann et al., 1987). Dipolar relaxation was studied as a function of temperature T via measurements of the complex dielectric susceptibility, $\chi = \chi' - i\chi''$ vs. T , by use of different experimental methods adapted to different frequency ranges, $10^{-3} \leq f \leq 10^6 \text{ Hz}$. They included a Solartron 1260 impedance analyzer with 1296 dielectric interface (Fig. 10a and b) and a digital lock-in analyzer (Wickenhöfer et al., 1991) (Fig. 10c) for linear, and a homemade computer-controlled digital susceptometer (Miga et al., 2007) for non-linear dielectric susceptibility data (Fig. 11) at high precision under relatively low excitation voltages.

Fig. 10a and b show dielectric susceptibility data, $\chi'(T)$ and $\chi''(T)$, for frequencies $10^{-3} < f < 10^6 \text{ Hz}$, which reveal various signatures of glassy behaviour. The peak of $\chi'(T)$ in Fig. 10a converges toward a finite glass temperature, $T_m \rightarrow T_g = (33.6 \pm 0.1) \text{ K}$ (Wickenhöfer et al., 1991) following critical dynamics with a power law $\tau = 1 / (2\pi f) = \tau_0 \varepsilon^{-z\nu}$, where $\varepsilon = (T_m / T_g - 1) > 0$ is the reduced temperature and $z\nu = 6.6 \pm 0.2$ is the dynamical critical exponent. Essentially the same (static) glass temperature, $T_g = (33.5 \pm 1.5) \text{ K}$, emerges for the

'largest' relaxation time τ_m as defined by the condition $\chi''(f_{\min}, T) = 0.05\chi''_{\max}(T)$ from frequency spectra of the loss function $\chi''(f)$ in Fig. 10c (Kleemann et al., 2011). In this figure it is clearly seen, how the center of gravity of the loss spectrum shifts to very low frequencies and its width broadens toward very long relaxation times, $\tau_m \rightarrow \infty$, as $T \rightarrow T_g$.

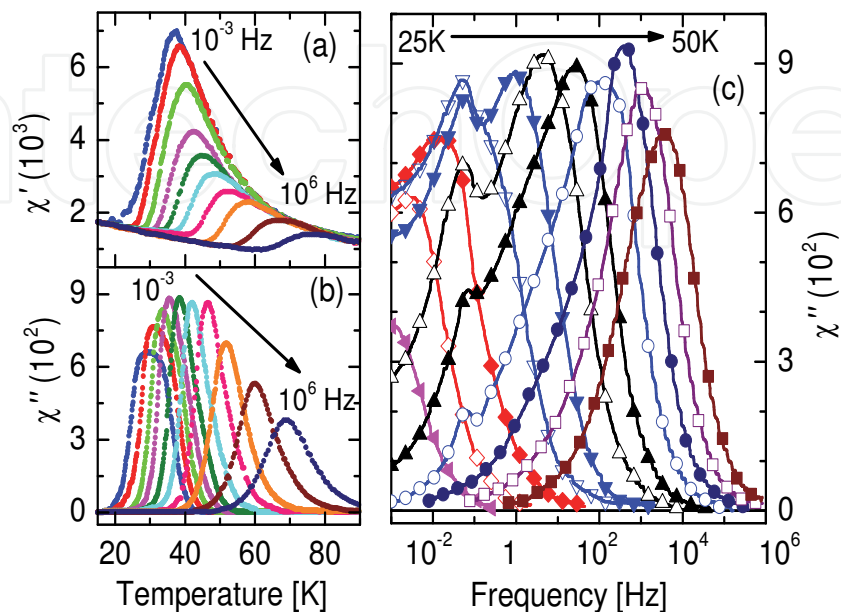


Fig. 10. Dielectric susceptibility, $\chi'(T)$ (a), $\chi''(T)$ (b), and $\chi''(f)$ (c) of $K_{0.989}Li_{0.011}TaO_3$ measured at frequencies $10^{-3} < f < 10^6$ Hz and temperatures $10 < T < 90$ K. Decades of f and steps of $\Delta T = 2.5$ K are parameters in (a, b) and (c), respectively.

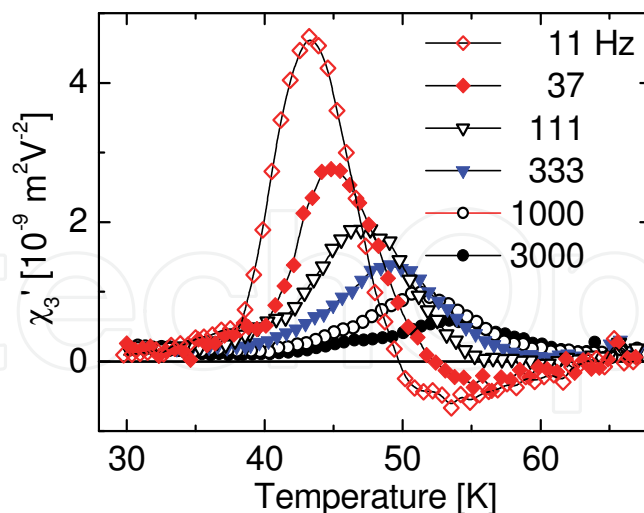


Fig. 11. Nonlinear susceptibility $\chi_3'(T)$ of $K_{0.989}Li_{0.011}TaO_3$ measured at frequencies $11 < f < 3000$ Hz.

A complementary test of glassy criticality refers to the third-order nonlinear susceptibility, $\chi_3' \propto \partial^3 P / \partial E^3$. It fulfils the expectation of a divergence at T_g (Binder & Reger, 1992) only partially. Fig. 11 shows χ_3' vs. T for frequencies $11 \text{ Hz} \leq f \leq 3 \text{ kHz}$ on cooling with

$dT/dt = -0.2\text{K/min}$ under an *ac* field amplitude $E_0 = 45 \text{ kV/m}$ and by analyzing the emerging signal up to the fifth harmonic (Kleemann et al., 2011). While χ'_3 drops below zero on the high- T edge at low frequencies, all signals are dominated by positive low- T peaks. This unexpected result is very probably due to the fact that the dipolar glass KLT is only insufficiently modeled by a pseudospin system in full analogy to an Ising spin glass (Binder & Reger, 1992). Actually we deal with a frustrated system of nanoclusters (Vugmeister & Glinchuk, 1990), which are subject to complex dipolar interactions and underlie internal dynamical degrees of freedom. As a consequence the nanodipolar clusters do not primarily flip under the external electric *ac* field, but merely change their shape and shift their centers of gravity in the sense of a breathing mode. Obviously this action becomes more effective the lower the temperature (*i.e.* the higher the lattice permittivity) and the lower the frequency. Thus the expected negative divergence is replaced by a positive peak nearly coinciding with that of the linear susceptibility, χ'_1 (Fig. 10a).

4.4.3 Multiglass $\text{Sr}_{0.98}\text{Mn}_{0.02}\text{TiO}_3$

The experiments on $\text{Sr}_{0.98}\text{Mn}_{0.02}\text{TiO}_3$ were performed on a ceramic sample prepared by a mixed oxide technology (Tkach et al., 2005). Preponderant incorporation of Mn^{2+} onto A-sites of the perovskite structure (Fig. 9) was confirmed by energy dispersive X-ray spectra (Tkach et al., 2006), Mn^{2+} ESR analysis (Laguta et al., 2007), and EXAFS spectroscopy (Lebedev et al., 2009; Levin et al., 2010). Fig. 12 shows the components of the complex dielectric susceptibility $\chi = \chi' - i\chi''$ recorded at frequencies $10^{-3} \leq f \leq 10^6 \text{ Hz}$ and temperatures $10 \leq T \leq 100 \text{ K}$ as $\chi'(T)$ (a) and $\chi''(f)$ (c). The broad and strongly frequency dependent peaks of both components are related to the dynamics of polar clusters created by off-center displacements of Mn^{2+} cations (Tkach et al., 2007). The position of the peak temperatures T_m in Fig. 12a is well described by a power law of the respective frequency, $f(T_m) \propto (T_m / T_g - 1)^{z\nu}$, which is a typical manifestation of glassy critical behavior (Shvartsman et al., 2008). Best fits of the experimental data yield the glass temperature $T_g = 38.3 \pm 0.3 \text{ K}$ (Fig. 12b) and the dynamical critical exponent, $z\nu = 8.5 \pm 0.2$, which compares well with that of spin glasses (Jönsson, 2004). Obviously the dynamics of the polar clusters becomes frozen at T_g , where the relaxation time $\tau = 1 / (2\pi f)$ diverges on a percolating network. This defines a PT from the disordered super-paraelectric to a cluster glass state. Similarities with superspin glass characteristics (Jönsson, 2004) are obvious. As described elsewhere (Shvartsman et al., 2008, Kleemann et al., 2009) this freezing process initiates also the transition of the Mn^{2+} spin moments into a spin glass state, which is magneto-electrically coupled to the dipolar glass state.

Another striking indicator of the dipolar glass state is the memory effect, which arises after isothermally annealing the sample below T_g . Fig. 12b shows an example of 'burning a hole' with depth $\Delta\chi'(T_w) = \chi'_{\text{wait}} - \chi'_{\text{ref}}(T_w) \approx -6$ at the wait temperature $T_w = 32.5 \text{ K}$ after waiting for $t_w \approx 10.5 \text{ h}$ (arrow). It signifies the asymptotic approach to the 'stiff' glassy ground state at T_w , which has the lowest susceptibility with respect to an external homogeneous field. Since the structure of the glassy ground state varies as a function of the temperature, the system is 'rejuvenating' at temperatures sufficiently far from T_w (Jönsson, 2004), hence, localizing the 'burnt hole' around T_w . This contrasts with the global decrease expected for an ordinarily relaxing metastable system.

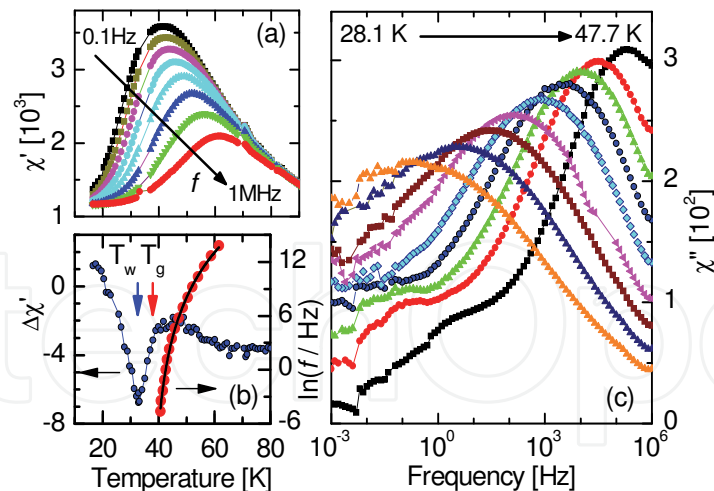


Fig. 12. (a) $\chi'(T)$ of $\text{Sr}_{0.98}\text{Mn}_{0.02}\text{TiO}_3$ recorded at $E_{ac} = 60$ V/m and frequencies $f = 10^{-1}, 10^0, 10^1, 10^2, 10^3, 10^4, 10^5$, and $0.4 \cdot 10^6$ Hz. (b) Frequency (f) dependence of the peak temperature (T_m) of $\chi'(T)$ taken from (a), plotted as $\ln(f/\text{Hz})$ vs. T_m , and fitted by a critical power law (solid line), and difference curve $\Delta\chi' = \chi'_{\text{wait}} - \chi'_{\text{ref}}$ vs. T obtained at $f = 10$ Hz and $E_{ac} = 60$ V/m upon heating after zero-field cooling from 80 K and waiting for 10.5 h at $T_w = 32.5$ K (χ'_{wait}) or without waiting (χ'_{ref}), respectively. T_g and T_w are marked by arrows. (c) $\chi''(f)$ as measured at frequencies $10^{-3} \leq f \leq 10^6$ Hz and temperatures $28.1 \leq T \leq 47.7$ K in 2.2 K steps.

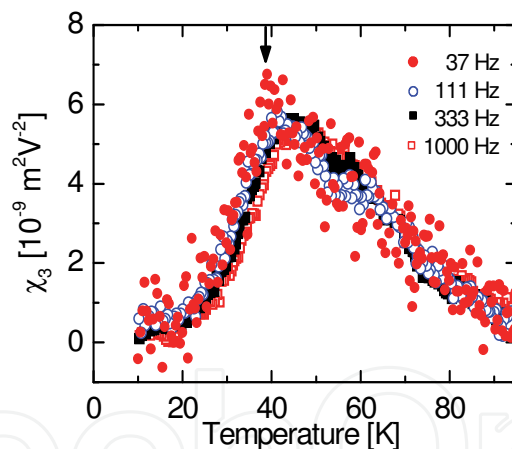


Fig. 13. Temperature dependence of the third-order nonlinear dielectric susceptibility of $\text{Sr}_{0.98}\text{Mn}_{0.02}\text{TiO}_3$ measured at $f = 37, 111, 333$ and 1000 Hz. The dipolar glass freezing temperature $T_g \approx 38$ K is indicated by a vertical arrow.

The glass transition may also be judged from spectra χ'' vs. $\log f$ (Shvartsman et al., 2008) similarly as shown for $\text{K}_{0.989}\text{Li}_{0.011}\text{TaO}_3$ (Fig. 10c). Since $\chi''(f)$ measures the distribution function of relaxation times, its extension over more than nine decades of frequencies clearly signifies the glassy nature of the system. At low frequencies, $f < 10^{-1}$ Hz, the low- f branch of $\chi''(T)$ is observed to gradually lift up and to become horizontal at $T < 38.9$ K. This suggests it to extend with finite amplitude to $f_{\text{min}} \rightarrow 0$, hence, $\tau_{\text{max}} \rightarrow \infty$ for the percolating glass cluster. Maybe the ultimate proof of the very existence of a generic dipolar glass is given by the dynamic nonlinear susceptibility $\chi_3 = (\partial^3 P / \partial E^3) / (6\epsilon_0)$ (Miga et al., 2007) in Fig. 13. This

seems to indicate a divergence as $T \rightarrow T_g$ and $f \rightarrow 0$ as predicted by theory (Binder & Reger, 1992), but has rarely been evidenced on orientational glasses (Hemberger et al., 1996). At the lowest frequency, $f = 37$ Hz, a fairly sharp peak is encountered, whose high- T branch might be considered as a critical hyperbola. Excess noise, however, prevents from seriously fitting a critical exponent, which should be close to $\gamma = 1$ as found previously (Hemberger et al., 1996). However, since the nonlinear susceptibility is modified by non-diverging ferroic (*viz.* ferroelectric) correlations due to progressive cluster formation on cooling, we cannot expect rigorous proportionality to the 'spin' glass susceptibility (Binder & Reger, 1992). Very probably the expected divergence is damped out similarly as in the case of KLT (Fig. 11).

5. Conclusion

In subsections 4.1 - 4.4 we presented different groups of polar materials separately and compared qualitatively their dielectric properties with predictions of suitable theories. It is likewise interesting to compare quantitatively different materials. The scaled nonlinear susceptibility, a_3 , is defined independently of the kind of material and its symmetry. This quantity is a measure of the nonlinearity of the investigated object. For an adequate comparison we have chosen values of a_3 within centrosymmetric phases of different materials close to their temperatures of phase transition or of peak positions of the linear susceptibility, respectively. Fig. 14 shows thus collected values of a_3 . In view of the very large differences between the different a_3 values a logarithmic scale is used. Consequently, only the magnitude values, $|a_3|$, are presented. The highest $|a_3|$ was found for Rochelle salt, RS. Lower nonlinearity appears in sequence in the ferroelectric crystals TGS, LGO, BT, barium doped LGO, multiglass $\text{Sr}_{0.98}\text{Mn}_{0.02}\text{TiO}_3$, orientational glass $\text{K}_{0.989}\text{Li}_{0.011}\text{TaO}_3$ and relaxor ferroelectrics PMN and SBN 61. Obviously, classic ferroelectrics undergoing continuous PT are characterized by high nonlinearity, while structural disorder and presence of PNRs diminish the nonlinearity. Consequently relaxor ferroelectrics are characterized by the smallest values of a_3 . In other words, displacive ferroelectrics exhibiting soft-mode softening are most affected by nonlinearity, while typical order-disorder systems do not obtain their ferroelectricity primarily from the nonlinear interionic potential. The mechanism of their phase transition rather reflects the statistics of local hopping modes, in particular when being accompanied by quenched random fields as in relaxor ferroelectrics (Westphal et al., 1992; Kleemann et al., 2002), but probably also in partial order-disorder systems like BaTiO_3 (Zalar et al., 2003).

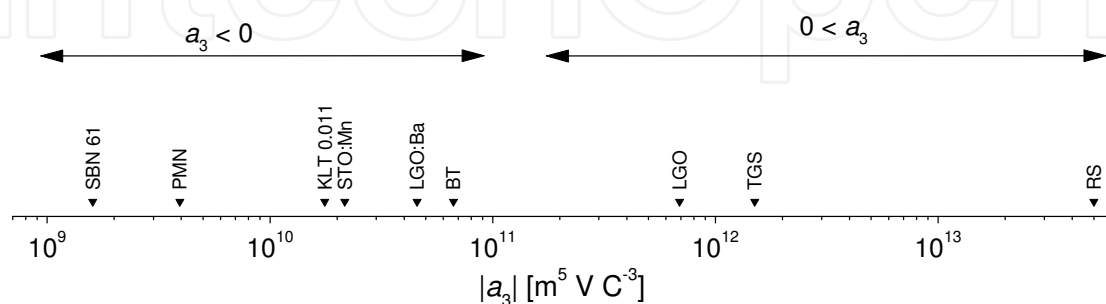


Fig. 14. Absolute values of the scaled nonlinear susceptibility, $|a_3|$, within centrosymmetric phases close to temperatures of phase transitions (for classic ferroelectrics) or peak positions of the linear susceptibility at low- f (for relaxor ferroelectrics and glasses).

The comparison of nonlinear dielectric response of various kinds of polar materials presented in this chapter gives evidence that such kind of measurement is a very sensitive tool for determination of the nature of ferroelectrics. Particularly useful for this purpose are the third-order dielectric susceptibility and the scaled non-linear susceptibility, a_3 . In our opinion, the second-order dielectric susceptibility is less significant, since it is more characteristic of the sample state than of a particular group of ferroelectrics. If anything, this susceptibility contains information about the distinct polar state of the sample. This information may be used for checking the presence of a center of inversion. The nonlinear dielectric response of classic ferroelectric crystals displaying continuous or discontinuous phase transition stays in a good agreement with predictions of the thermodynamic theory of ferroelectric phase transition. Predictions of the scaling theory for TGS crystal are also successfully verified experimentally. The situation is much more complex in disordered systems like ferroelectric relaxors or dipolar glasses. Respective theories properly explaining the observed features have still to be developed and tested via dynamic nonlinear dielectric response.

6. Acknowledgment

The authors are grateful to D. Rytz, A. Tkach, and P.M. Vilarinho for providing samples. WK thanks the Foundation for Polish Science (FNP), Warsaw, for an Alexander von Humboldt Honorary research grant.

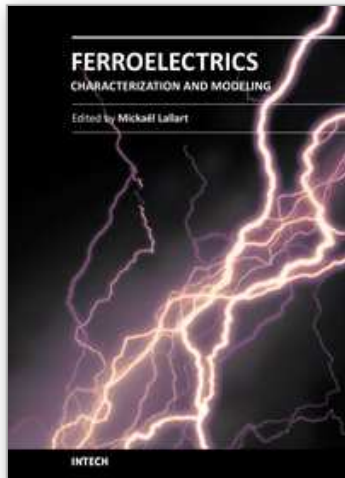
7. References

- Binder, K. & Reger, J. D. (1992). Theory of orientational glasses: models, concepts, simulations, *Adv. Phys.*, Vol. 41, pp. 547 - 627
- Binder, K. & Young, A. P. (1986). Spin glasses: Experimental facts, theoretical concepts, and open questions, *Rev. Mod. Phys.*, Vol. 58, pp. 801 - 976
- Bobnar, V., Kutnjak, Z., Pirc, R., Blinc, R., & Levstik, A. (2000). Crossover from glassy to inhomogeneous-ferroelectric nonlinear dielectric response in relaxor ferroelectrics, *Phys. Rev. Lett.*, Vol. 84, pp. 5892 - 5895
- Bonneau, P., Garnier, P., Calvarin, G., Husson, E., Gavarrri, J. R., Hewat, A. W. & Morell, A. (1991). X-ray and neutron diffraction studies of the diffuse phase transition in $\text{PbMg}_{1/3}\text{Nb}_{2/3}\text{O}_3$ ceramics, *J. Solid State Chem.*, Vol. 91, pp. 350-361
- Böttcher, C. J. F. (1973). *Theory of Electric Polarization*, Elsevier, Amsterdam, Oxford, New York
- Burns, G. & Dacol, F. H. (1983). Crystalline ferroelectrics with glassy polarization behavior, *Phys. Rev. B*, Vol. 28, pp. 2527 - 2530
- Cach, R. (1988). Time changes of the internal bias field in γ -damaged TGS crystal, *Acta Univ. Wratislaviensis*, Vol. 1084, pp. 125 - 133
- Chen, A. & Zhi, Y. (2004). DC electric-field dependence of the dielectric constant in polar dielectrics: "multi-polarization-mechanism" model, *Phys. Rev. B*, Vol. 69, p. 174109-1 - 174109-8
- Debye, P. (1929). *Polar Molecules*, The Chemical Catalog Company, Inc., New York
- Dec, J., Miga, S., Kleemann, W. & Dkhil, B. (2008). Nonlinear dielectric properties of PMN relaxor crystals within Ginzburg-Landau-Devonshire approximation, *Ferroelectrics*, Vol. 363, p. 141 - 149

- Dec, J., Miga, S., Trybuła, Z., Kaszyńska, K. & Kleemann, W. (2010). Dynamics of Li⁺ dipoles at very low concentration in quantum paraelectric potassium tantalate, *J. Appl. Phys.*, Vol. 107, p. 094102-1 - 094102-8
- Devonshire, A. F. (1949). Theory of barium titanate, Part I, *Phil. Mag.*, Vol. 40, pp. 1040 - 1063
- Fisher, D. S (1986). Scaling and critical slowing down in random-field Ising systems, *Phys. Rev. Lett.*, Vol. 56, p. 416 - 419
- Fujimoto, M. (2003). *The physics of structural phase transitions* (2nd ed.), Springer-Verlag, Berlin, Heidelberg, New York
- Ginzburg, V. L. (1945). On the dielectric properties of ferroelectric (Seignetteelectric) crystals and barium titanate, *Zh. Exp. Theor. Phys.*, Vol. 15, pp. 739 - 749
- Glazounov, A. E. & Tagantsev, A. K. (2000). Phenomenological model of dynamic nonlinear response of relaxor ferroelectrics, *Phys. Rev. Lett.* vol. 85, pp. 2192-2195
- Hemberger, J., Ries, H., Loidl, A. & Böhmer, R. (1996). Static freezing transition at a finite temperature in a quasi-one-dimensional deuteron glass, *Phys. Rev. Lett.*, Vol. 76, pp. 2330 - 2333
- Höchli, U. T. (1982). Dynamics of freezing electric dipoles, *Phys. Rev. Lett.*, Vol. 48, pp. 1494 - 1497
- Höchli, U. T., Knorr, K. & Loidl, A. (1990). Orientational glasses, *Advan. Phys.*, Vol. 39, pp. 405 - 615
- Ikeda, S., Kominami, H., Koyama, K. & Wada, Y. (1987). Nonlinear dielectric constant and ferroelectric-to-paraelectric phase transition in copolymers of vinylidene fluoride and trifluoroethylene, *J. Appl. Phys.*, Vol. 62, pp. 3339 - 3342
- Jönsson, P.E. (2004). Superparamagnetism and spin-glass dynamics of interacting magnetic nanoparticle systems, *Adv. Chem. Phys.*, Vol. 128, pp. 191 - 248
- Jonscher A. K. (1983). *Dielectric Relaxation in Solids*, Chelsea Dielectrics, London
- Kleemann, W., Kütz, S. & Rytz, D. (1987). Cluster glass and domain state properties of KTaO₃:Li, *Europhys. Lett.*, Vol. 4, pp. 239 - 245
- Kleemann W., Dec J., Lehnen P., Blinc R., Zalar B., and Pankrath R. (2002). Uniaxial relaxor ferroelectrics: the ferroic random-field Ising model materialized at last, *Europhys. Lett.*, Vol. 57, pp. 14 - 19
- Kleemann, W., Shvartsman, V.V., Bedanta, S., Borisov, P., Tkach, A. & Vilarinho, P. M. (2008). (Sr,Mn)TiO₃ - a magnetoelectrically coupled multiglass, *J. Phys.: Condens. Matter*, Vol. 20, pp. 434216-1 - 434216-6
- Kleemann, W., Bedanta, S., Borisov, P., Shvartsman, V. V., Miga, S., Dec, J., Tkach, A. & Vilarinho, P.M. (2009). Multiglass order and magnetoelectricity in Mn²⁺ doped incipient ferroelectrics, *Eur. Phys. J. B*, Vol. 71, pp. 407 - 410
- Kleemann, W., Dec, J., Miga, S. & Rytz, D. (2011). Polar states of the impurity system KTaO₃:Li, *Z. Kristallogr.* Vol. 226, pp. 145 - 149
- Kremer, F. & Schönhal, A. (Eds.). (2003). *Broadband Dielectric Spectroscopy*, Springer-Verlag, Berlin, Heidelberg, New York
- Laguta, V. V., Kondakova, I. V., Bykov, I. P., Glinchuk, M. D., Tkach, A., Vilarinho, P. M. & Jastrabik, L. (2007). Electron spin resonance investigation of Mn²⁺ ions and their dynamics in Mn-doped SrTiO₃, *Phys. Rev. B*, Vol. 76, pp. 054104-1 - 054104-6
- Lebedev, A. I., Sluchinskaja, I. A., Erko, A. & Kozlovskii, A. F. (2009). Direct evidence for off-centering of Mn impurity in SrTiO₃, *JETP-Lett.*, Vol. 89, pp. 457 - 467

- Leont'ev, I. N., Leiderman, A., Topolov, V. Yu. & Fesenko, O. E. (2003). Nonlinear properties of barium titanate in the electric field range $0 \leq E \leq 5.5 \times 10^7$ V/m, *Phys. Solid State*, Vol. 45, pp. 1128-1130
- Levin, I., Krayzman, V., Woicik, J. C., Tkach, A. & Vilarinho, P. M. (2010). X-ray absorption fine structure studies of Mn coordination in doped perovskite SrTiO₃, *Appl. Phys. Lett.*, Vol. 96, pp. 052904-1 - 052904-3
- Lines, M. E. & Glass, A. M. (1977). *Principles and Applications of Ferroelectrics and Related Materials*, Oxford University Press, London
- Mierzwa, W., Fugiel, B. & Ćwikiel, K. (1998). The equation-of-state of triglycine sulphate (TGS) ferroelectric for both phases near the critical point, *J. Phys.: Condens. Matter*, Vol. 10, pp. 8881 - 8892
- Miga, S., Dec, J., Molak, A. & Koralewski, M. (2006). Temperature dependence of nonlinear susceptibilities near ferroelectric phase transition of a lead germanate single crystal, *J. Appl. Phys.*, Vol. 99, pp. 124107-1 - 124107-6
- Miga, S., Dec, J. & Kleemann, W. (2007). Computer-controlled susceptometer for investigating the linear and non-linear dielectric response, *Rev. Sci. Instrum.*, Vol. 78, pp. 033902-1 - 033902-7
- Miga, S. & Dec, J. (2008). Non-linear dielectric response of ferroelectric and relaxor materials, *Ferroelectrics*, Vol. 367, p. 223 - 228
- Miga, S., Dec, J., Molak, A. & Koralewski, M. (2008). Barium doping-induced polar nanoregions in lead germanate single crystal, *Phase Trans.*, Vol. 81, pp. 1133 -1140
- Miga, S., Czaplak, Z., Kleemann, W. & Dec, J. (2010a). Non-linear dielectric response in the vicinity of the 'inverse melting' point of Rochelle salt, *Ferroelectrics*, Vol. 400, p. 76-80
- Miga, S., Kleemann, W. & Dec J. (2010b). Non-linear dielectric susceptibility near to the field-induced ferroelectric phase transition of $K_{0.937}Li_{0.063}TaO_3$, *Ferroelectrics*, Vol. 400, p. 35 - 40
- Mitsui, T. (1958). Theory of the ferroelectric effect in Rochelle salt, *Phys. Rev.*, Vol. 111, pp. 1259 - 1267
- Oliver, J. R., Neurgaonkar, R. R. & Cross, L. E. (1988). A thermodynamic phenomenology for ferroelectric tungsten bronze Sr_{0.6}Ba_{0.4}Nb₂O₆ (SBN:60), *J. Appl. Phys.*, Vol.64, pp. 37-47
- Pirc, R., Tadić, B. & Blinc, R. (1994). Nonlinear susceptibility of orientational glasses, *Physica B*, Vol. 193, pp. 109 - 115
- Pirc, R. & Blinc, R. (1999). Spherical random-bond-random-field model of relaxor ferroelectrics, *Phys. Rev. B*, Vol. 60, pp. 13470 - 13478
- Shvartsman, V. V., Bedanta, S., Borisov, P., Kleemann, W., Tkach, A. & Vilarinho, P. (2008). (Sr,Mn)TiO₃ - a magnetoelectric multiglass, *Phys. Rev. Lett.*, Vol. 101, pp. 165704-1 - 165704-4
- Smolenskii, G. A., Isupov, V. A., Agranovskaya, A. I. & Popov, S. N. (1960). Ferroelectrics with diffuse phase transition (in Russian), *Sov. Phys. -Solid State*, Vol. 2, pp. 2906-2918
- Stanley, H. E. (1971). *Introduction to Phase Transitions and Critical Phenomena*, Clarendon, Oxford

- Tkach, A., Vilarinho, P. M. & Kholkin, A. L. (2005). Structure-microstructure-dielectric tunability relationship in Mn-doped strontium titanate ceramics, *Acta Mater.*, Vol. 53, pp. 5061- 5069
- Tkach, A., Vilarinho, P. M. & Kholkin, A. L. (2006). Dependence of dielectric properties of manganese-doped strontium titanate ceramics on sintering atmosphere, *Acta Mater.*, Vol. 54, pp. 5385 - 5391
- Tkach, A., Vilarinho, P. M. & Kholkin, A. L. (2007). Non-linear dc electric-field dependence of the dielectric permittivity and cluster polarization of $\text{Sr}_{1-x}\text{Mn}_x\text{TiO}_3$ ceramics, *J. Appl. Phys.*, Vol. 101, pp. 084110-1 - 084110-9
- Valasek, J. (1920). Piezoelectric and allied phenomena in Rochelle salt, *Phys. Rev.*, Vol. 15, pp. 537 - 538
- Valasek, J. (1921). Piezo-electric and allied phenomena in Rochelle salt, *Phys. Rev.*, Vol. 17, pp. 475 - 481
- von Hippel, A. (1950). Ferroelectricity, domain structure, and phase transitions of barium titanate, *Rev. Mod. Phys.*, Vol. 22, pp. 222 - 237
- von Hippel, A. (1954). *Dielectrics and Waves*, Wiley, New York
- Vugmeister, B. E. & Glinchuk, M. D. (1990). Dipole glass and ferroelectricity in random-site electric dipole systems, *Rev. Mod. Phys.*, Vol. 62, pp. 993 - 1026
- Wang, Y. L., Tagantsev, A. K., Damjanovic, D. & Setter, N. (2006). Anharmonicity of BaTiO_3 single crystals, *Phys. Rev. B*, Vol. 73, pp. 132103-1 - 132103-4
- Wang, Y. L., Tagantsev, A. K., Damjanovic, D., Setter, N., Yarmarkin, V. K., Sokolov, A. I. & Lukyanchuk, I. A. (2007). Landau thermodynamic potential for BaTiO_3 , *J. Appl. Phys.*, Vol. 101, pp. 104115-1 - 104115-9
- Wei, X. & Yao, X. (2006a). Reversible dielectric nonlinearity and mechanism of electrical tunability for ferroelectric ceramics, *Int. J. Mod. Phys. B*, Vol. 20, p. 2977 - 2998
- Wei, X. & Yao, X. (2006b). Analysis on dielectric response of polar nanoregions in paraelectric phase of relaxor ferroelectrics, *J. Appl. Phys.*, Vol. 100, p. 064319-1 - 064319-6
- Westphal, V., Kleemann, W. & Glinchuk, M. (1992). Diffuse phase transitions and random field-induced domain states of the "relaxor" ferroelectric $\text{PbMg}_{1/3}\text{Nb}_{2/3}\text{O}_3$, *Phys. Rev. Lett.*, Vol. 68, pp. 847 - 950
- Wickenhöfer, F., Kleemann, W. & Rytz, D. (1991). Dipolar freezing of glassy $\text{K}_{1-x}\text{Li}_x\text{TaO}_3$, $x = 0.011$, *Ferroelectrics*, Vol. 124, pp. 237 - 242
- Zalar, B., Laguta, V. V. & Blinc, R. (2003). NMR evidence for the coexistence of order-disorder and displacive components in barium titanate, *Phys. Rev. Lett.*, Vol. 90, pp. 037601-1 - 037601-4



Ferroelectrics - Characterization and Modeling

Edited by Dr. Mickaël Lallart

ISBN 978-953-307-455-9

Hard cover, 586 pages

Publisher InTech

Published online 23, August, 2011

Published in print edition August, 2011

Ferroelectric materials have been and still are widely used in many applications, that have moved from sonar towards breakthrough technologies such as memories or optical devices. This book is a part of a four volume collection (covering material aspects, physical effects, characterization and modeling, and applications) and focuses on the characterization of ferroelectric materials, including structural, electrical and multiphysic aspects, as well as innovative techniques for modeling and predicting the performance of these devices using phenomenological approaches and nonlinear methods. Hence, the aim of this book is to provide an up-to-date review of recent scientific findings and recent advances in the field of ferroelectric system characterization and modeling, allowing a deep understanding of ferroelectricity.

How to reference

In order to correctly reference this scholarly work, feel free to copy and paste the following:

Seweryn Miga, Jan Dec and Wolfgang Kleemann (2011). Non-Linear Dielectric Response of Ferroelectrics, Relaxors and Dipolar Glasses, *Ferroelectrics - Characterization and Modeling*, Dr. Mickaël Lallart (Ed.), ISBN: 978-953-307-455-9, InTech, Available from: <http://www.intechopen.com/books/ferroelectrics-characterization-and-modeling/non-linear-dielectric-response-of-ferroelectrics-relaxors-and-dipolar-glasses>

INTECH
open science | open minds

InTech Europe

University Campus STeP Ri
Slavka Krautzeka 83/A
51000 Rijeka, Croatia
Phone: +385 (51) 770 447
Fax: +385 (51) 686 166
www.intechopen.com

InTech China

Unit 405, Office Block, Hotel Equatorial Shanghai
No.65, Yan An Road (West), Shanghai, 200040, China
中国上海市延安西路65号上海国际贵都大饭店办公楼405单元
Phone: +86-21-62489820
Fax: +86-21-62489821

© 2011 The Author(s). Licensee IntechOpen. This chapter is distributed under the terms of the [Creative Commons Attribution-NonCommercial-ShareAlike-3.0 License](#), which permits use, distribution and reproduction for non-commercial purposes, provided the original is properly cited and derivative works building on this content are distributed under the same license.

IntechOpen

IntechOpen